

# Ferritic nitrocarburising of tool steels

P. C. King<sup>\*1</sup>, R. W. Reynoldson<sup>2</sup>, A. Brownrigg<sup>1</sup> and J. M. Long<sup>1</sup>

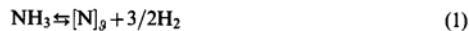
Four different tool steel materials, P20, H13, M2 and D2, were nitrocarburised at 570°C in a fluidised bed furnace. The reactive diffusion of nitrogen and carbon into the various substrate microstructures is compared and related to the different alloy carbide distributions. The effect of carbon bearing gas (carbon dioxide, natural gas) on carbon absorption is reported, as well as its influence on compound layer growth and porosity. Partial reduction of Fe<sub>3</sub>O<sub>4</sub> at the surface resulted in the formation of a complex, ε-nitride containing oxide layer. In H13, carbon was deeply absorbed throughout the entire diffusion zone, affecting the growth of grain boundary cementite, nitrogen diffusivity and the sharpness of the compound layer: diffusion zone interface. When natural gas was used, carbon became highly concentrated in the compound layer, while surface decarburisation occurred with carbon dioxide. These microstructural effects are discussed in relation to hardness profiles, and compound layer hardness and ductility. The surfaces were characterised using glow discharge optical emission spectroscopy, optical and scanning electron microscopy and X-ray diffraction.

**Keywords:** Nitrocarburising, Tool steel: H13, M2, D2, P20, Reactive diffusion, GD-OES, Cover layer, Compound layer, Diffusion zone, porosity, Fluidised bed, SEM, XRD

## Introduction

Ferritic nitrocarburising is a thermochemical surface treatment involving the simultaneous diffusion of nitrogen and carbon into a steel surface at ~570–580°C. It is performed primarily to improve the wear resistance and fatigue strength of ferrous components. Compared with other treatments, nitrocarburising stands out as simple, cheap and offering improvements over a range of properties. Workpieces do not suffer the same degree of distortion as takes place during high temperature treatments, which can lead to expensive regrinding of intricate die cavities or, in some cases, even rejection of the component. Treatment times are a fraction of those needed for nitriding, and therefore nitrocarburising offers an alternative so long as the shallower case depth is not a concern.

Nitrocarburising gas atmospheres consist of a nitrogen bearing gas (ammonia), a carbon bearing gas and an inert carrier gas (usually N<sub>2</sub>). The choice of carbon bearing component varies, propane, endothermic gas and carbon dioxide all being typical examples. Nitrogen adsorption from the gas phase and dissolution into surface phase  $\phi$  occurs owing to the partial dissociation of ammonia.<sup>1–3</sup>



The principal measure of the driving force for nitrogen

diffusion imposed by the gaseous atmosphere is the nitrogen activity  $a_{\text{N}}$ , which is derived directly from the expression for the equilibrium constant  $K_{(1)}$  of equation (1).

$$a_{\text{N}} = K_{(1)} \frac{p_{\text{NH}_3}}{(p_{\text{H}_2})^{3/2}} \quad (2)$$

where  $p_j$  denotes the partial pressure of gas component  $j$ .

When CO<sub>2</sub> is used as the carbon bearing gas, reaction with H<sub>2</sub> (a product of ammonia dissociation) forms carbon monoxide according to the homogeneous water-gas reaction (3). Carbon monoxide delivers nascent carbon to the workpiece surface according to reaction (4), the heterogeneous water-gas reaction.



The carbon activity is derived directly from the expression for the equilibrium constant  $K_{(4)}$  of reaction (4).

$$a_{\text{C}} = K_{(4)} \frac{p_{\text{CO}}p_{\text{H}_2}}{p_{\text{H}_2\text{O}}} \quad (5)$$

If the carbon bearing gas contains methane, carbon is produced by direct dissociation.<sup>4</sup>



Many components for nitrocarburising are made of plain carbon steel. This is evident from the number of automotive parts that are routinely nitrocarburised.<sup>5–8</sup> However, other alloyed steels, including tool steels, are also of great importance. Hot working die steel, in

<sup>1</sup>School of Engineering and Technology, Deakin University, 221 Burwood Highway, Burwood, Vic. 3125, Australia

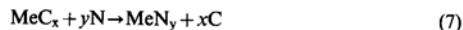
<sup>2</sup>Reynoldson Technologies, 160 Wickhams Rd, Launching Place, Vic. 3139, Australia

\*Corresponding author, email pckin@yahoo.com

particular the chromium–molybdenum type such as H13, is often nitrided or nitrocarburised for high pressure die casting tools.<sup>9</sup> H13 aluminium extrusion dies can also be nitrocarburised to improve die life. Components for the processing of polymers for the chemical, medical and foodstuffs industry require high corrosion resistance owing to attack from acids and chlorides formed from the decomposition of thermoplastics such as PVC. Die wear is a major problem, particularly during the manufacture of glass/ceramic phase reinforced polymers, and causes deterioration in product quality and possibly even significant downtime.<sup>10,11</sup> Cutting tools made of high speed steel can be nitrocarburised to allow for better retention of a sharp edge. However, here shorter cycle times are employed to prevent embrittlement.<sup>12,13</sup>

During nitrocarburising of iron or plain carbon steel, nitrogen diffuses into the surface as an interstitial solid solution of nitrogen in ferrite. This region of  $\alpha$  solid solution is known as the diffusion zone. At the very surface where the nitrogen concentration is the highest, the compound layer forms. This is also often referred to as the white layer, owing to its ability to withstand etching by nital. On plain carbon steel, it is composed of one or both of two iron carbonitrides,  $\epsilon$ -Fe<sub>2-3</sub>(N,C) and  $\gamma'$ -Fe<sub>4</sub>(N,C), and often includes some cementite Fe<sub>3</sub>C. The compound layer and diffusion zone dimensions vary according to the composition of the substrate, nitrogen and carbon activity and treatment temperature and time. However, 10–20  $\mu\text{m}$  is a typical compound layer thickness, while the diffusion zone is often >100  $\mu\text{m}$  deep. The compound layer imparts high hardness and wear resistance to the treated component and can also improve corrosion properties. When sufficiently rapidly quenched, the diffusion zone is responsible for improved fatigue properties. Typical nitrocarburising treatment times are 3–4 h at 570°C, compared with 24–72 h for nitriding at 500–550°C.

In alloy or tool steels, the diffusion zone is also capable of very high hardnesses, owing to the heavy dispersion of alloy nitrides which form when alloy carbides interact with inward diffusing nitrogen.<sup>14</sup>



Reactive diffusion of nitrogen with alloy carbides has been given a certain amount of attention for various nitriding processes,<sup>15–17</sup> but very little for nitrocarburising. During nitriding of some alloys, for instance, it has been found that coarse chromium and titanium carbides do not provide nucleation sites for nitride precipitation, but may partially redissolve in order to allow the nucleation and growth of alloy nitrides.<sup>18</sup> In other studies, fine intralath cementite was found to dissolve, while coarser lath boundary cementite acted as a nucleus for CrN, which then replaced it *in situ*.<sup>19</sup>

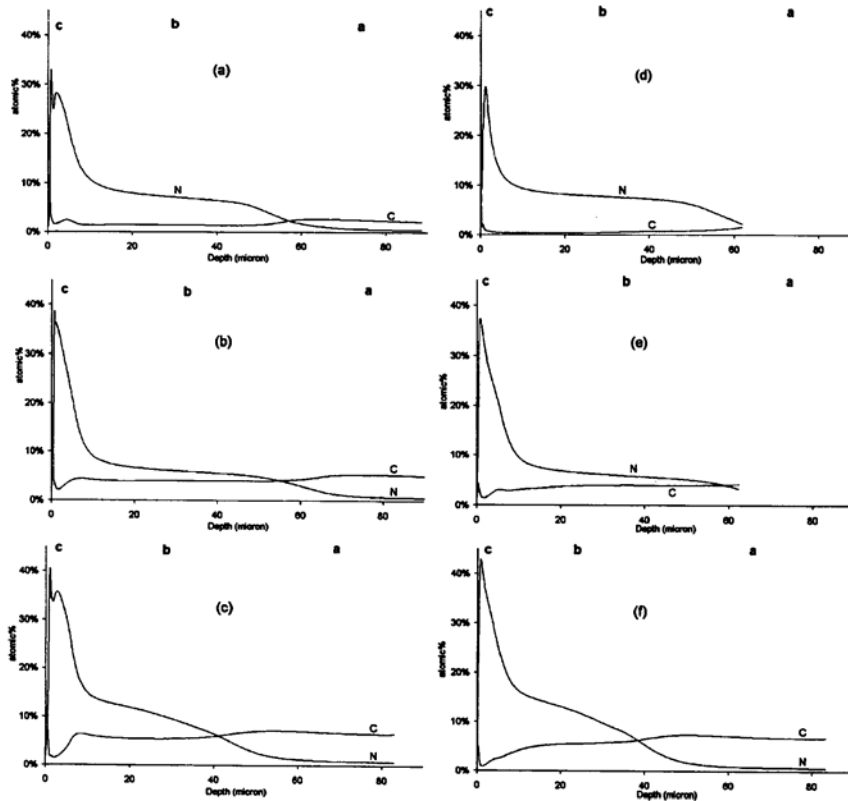
Carbon released by reaction (7) is pushed ahead by the transformation front. It diffuses inwards, forming carbides below the diffusion zone and creating a carbon enriched zone.<sup>19</sup> Carbon released by carbide dissolution also diffuses to prior austenite grain boundaries within the diffusion zone, forming cementite. There is a tendency for cementite to form mainly at those grain boundaries that are parallel to the surface, because a lower compressive stress acts in their growth direction. From torsion tests on ion nitrided steel, Edenhofer

found that diffusion zones that were largely free from grain boundary cementite were less embrittled than those with extensive Fe<sub>3</sub>C formation.<sup>20</sup> During nitrocarburising, the proportion of cementite increases towards the surface. Grain boundary cementite just beneath the compound layer can be converted to  $\epsilon$  phase. This usually links up with the compound layer and can be interpreted as if the compound layer had penetrated the grain boundaries of the diffusion zone.<sup>14</sup>

During nitrocarburising of tool steels, carbon released by reaction (7) as well as the carbon potential of the atmosphere destabilises  $\gamma'$ -Fe<sub>4</sub>(N,C).  $\epsilon$ -Fe<sub>2-3</sub>(N,C), in contrast, exists over a broad range of nitrogen and carbon solubility.<sup>21,22</sup> Compound layers with  $\epsilon$ -phase approaching 100% of the total volume possess superior scuffing and wear resistance to dual  $\gamma'$ + $\epsilon$  layers.<sup>23</sup> Other properties also influence the wear and corrosion behaviour, such as the extent of porosity, surface oxidation, the thickness of the compound layer and the level of carbon enrichment.

Nitrocarburised compound layers are characterised by porosity near the outer surface. Although porosity can be reduced by employing lower nitrogen activities, adjusting the carbon activity or temperature or limiting the treatment time (i.e. to moderate development of the compound layer itself), porosity is ultimately unavoidable.<sup>24</sup> In 1964, Mitchell and Dawes showed convincingly that porous nitrocarburised layers on mild steel are able to retain an oil film in lubricant starved conditions.<sup>12</sup> The lubricant retention ability of porous compound layers has since become a basic assumption of nitrocarburising. However, this is also dependent on the type of porosity that forms (e.g. whether pore channels open out to the exterior surface: columnar versus sponge type pore structure), and has yet to be proved on tool steels.

Another feature of the nitrocarburised surface is a certain degree of oxidation that occurs during the process. While nitriding usually involves subsequent removal of the whole compound layer unless the process itself is controlled to limit compound layer formation,<sup>25,26</sup> nitrocarburised components are frequently put into service without any post-machining, because the surface layers that are formed are not considered to be detrimental. After nitrocarburising, the parts have a dull, oxidised appearance. Moreover, many proprietary methods include additional post-nitrocarburising steps, such as water vapour treatment to form a protective Fe<sub>2</sub>O<sub>4</sub> layer, and immersion in organic sealant, to improve corrosion properties.<sup>27–29</sup> This, of course, depends on the application. Plastic moulding dies, for instance, require a bright polish, to achieve a good finish on the product. Nitrocarburising has also recently been investigated as a pretreatment for vapour deposited hard coatings, and it was found that oxides and porosity are hindrances in this situation.<sup>30,31</sup> In any event, oxygen in the treatment atmosphere plays an important role, because it acts as a catalyst for  $\epsilon$ -phase formation.<sup>23</sup> Thick compound layers can therefore be produced by nitrocarburising, with short treatment times compared with nitriding, using endothermic gas or carbon dioxide as the carbon bearing component of the mixture, owing to the high oxygen potential imparted by these gases. Work at low pressures has shown that oxygen aids in the formation of consistent layers.<sup>32</sup>



a H13, 25%NH<sub>3</sub>/16%CO<sub>2</sub>; b M2, 25%NH<sub>3</sub>/16%CO<sub>2</sub>; c D2, 25%NH<sub>3</sub>/16%CO<sub>2</sub>; d H13, 25%NH<sub>3</sub>, no carbon bearing gas; e M2, 25%NH<sub>3</sub>, no carbon bearing gas; f D2, 25%NH<sub>3</sub>, no carbon bearing gas  
 1 Carbon and nitrogen depth profiles through entire surface region affected by diffusion on various substrates nitrocarburised for 1 at 570°C

It is not clear from the literature to what extent carbon is absorbed by the substrate when various carbon bearing gases are used. Even less clear is the effect this has on the properties. Ebersbach *et al.*<sup>33</sup> found that the corrosion rate in a neutral 0.9M NaCl solution was an order of magnitude lower for  $\epsilon$ -carbonitride than for  $\epsilon$ -nitride. Polarisation curves showed that the onset of pitting was also shifted to higher potentials for  $\epsilon$ -carbonitride compared with the nitride phases. Meanwhile, porosity increased the uniform corrosion current owing to a larger surface area exposed to the solution. In contrast, Dawes *et al.*<sup>7</sup> found no difference in corrosion resistance between gas nitrided and nitrocarburised layers due to the presence of carbon. Hardness, scuffing and wear resistance were also found to be unaffected. There was a marginal improvement in

corrosion resistance after oil quenching (compared with air cooling) due to the retention of oil in the surface pores of the compound layer. However, Dawes' findings also contradicted those of Leroux,<sup>34</sup> who concluded that the greater the amount of carbon in  $\epsilon$ -Fe<sub>2-3</sub>(N,C), the harder the layer. Prenosi<sup>35</sup> stated that high carbon epsilon carbonitride layers formed using 50% ammonia and 50% propane had improved wear and scuffing resistance compared with epsilon nitride layers.

In the present study, tool steel materials were nitrocarburised in a fluidised bed furnace. In the fluidised bed, nitrogen, carbon and oxygen potentials are imposed by the same gaseous reactions as in a conventional gas furnace. However, higher nitrogen activities are common owing to the high gas velocity needed to fluidise the bed, which results in a lower

Table 1 Compositions of ferrous sample materials as determined by glow discharge optical emission spectrometry (GD-OES) bulk analysis, wt-%

AISI-SAE	Description	C	Mn	Si	Cr	Mo	V	W	Ni	Co	Cu
P20	Plastic mould steel	0.35	1.4	0.4	2.0	0.2	--	--	1.2	--	0.2
H13	Hot-working die steel	0.38	0.4	1.1	4.8	1.2	0.7	--	0.2	0.1	0.1
M2	High speed steel	1.03	0.2	0.3	3.9	4.4	1.5	5.9	0.5	0.7	0.3
D2	Cold working die steel	1.54	0.4	0.3	12.6	0.7	0.8	0.2	0.3	0.1	--

residence time of ammonia in the furnace chamber.<sup>36</sup> Other differences, such as the relationship between inlet ammonia level and nitrogen activity have been discussed elsewhere.<sup>37</sup> The ammonia level has been kept constant at 25% of total inlet flow. The study focuses on the reactive diffusion of nitrogen and carbon in four common tool steels during nitrocarburising. The role of carbon dioxide is discussed and compared with gas mixtures without a carbonaceous component, and then with atmospheres employing natural gas. Differences in compound layer development, shape of the diffusion profile and accrual of subsurface hardness are related to the final mechanical properties of the nitrocarburised layers.

## Experimental method

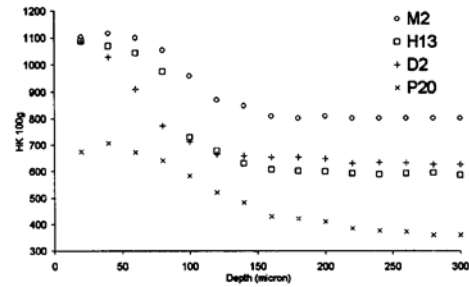
Four tool steel materials were chosen. Table 1 shows their composition, and Table 2 shows the heat treatment parameters. The samples were then nitrocarburised in an industrial 160 mm dia. fluidised bed at 570°C, with a total inlet flow of 1.5 m<sup>3</sup> h<sup>-1</sup>. P120-grit Al<sub>2</sub>O<sub>3</sub> powder (mean dia. 100 µm) was used as the fluidising medium. All samples were quenched in a second bed, fluidised with N<sub>2</sub> gas at ambient temperature. Various treatment times from 1 to 6 h were investigated, with three different types of treatment atmosphere: N<sub>2</sub>/25%NH<sub>3</sub>/8–16%CO<sub>2</sub>, N<sub>2</sub>/25%NH<sub>3</sub>, and N<sub>2</sub>/25%NH<sub>3</sub>/5–30% natural gas. For treatments using natural gas, this was sourced from the mains. Analysis provided by the refinery showed that the principal species were CH<sub>4</sub> 91.3–91.7%, C<sub>2</sub>H<sub>6</sub> 5.0–5.3%, CO<sub>2</sub> 1.9–2.1%.<sup>38</sup>

Optical microscopy was performed on mounted and polished cross-sections, both unetched and etched with nital. Images were also obtained on polished as well as fractured (unmounted) specimens by SEM. The LEO 1530 FEG SEM was operated on secondary electron mode at accelerating voltages of 5–10 kV and working distances of 10–15 mm.

Knoop microhardness indentations were performed on polished cross-sections at various depths from the surface (hardness profiling) using a 100 g load and 10 s dwell time, and 200 g Knoop microindentations and 5 kg Vickers macroindentations were also made directly on the treated surface, as described below.

X-ray diffraction (XRD) was performed with a Philips PW 1130/90 diffractometer at 40 kV, 25 mA, using a Ni filter. Cu K<sub>α</sub> radiation was used to probe the surface structure, because Cu K<sub>α</sub> only penetrates a few microns into the most common ferrous phases. The scan rate was 1° min<sup>-1</sup>, and step size 0.05°.

Depth profiles were obtained by GD-OES using a LECO GDS-850A instrument. Argon ions, excited by a dc voltage, sputtered a 4 mm dia. area of the sample surface. The displaced matter was analysed simultaneously by dual emission spectrometers, creating an elemental depth profile. The sample surfaces were not cleaned in any



2 Knoop microhardness depth profiles of four substrate materials following nitrocarburising for 3 h with N<sub>2</sub>/25%NH<sub>3</sub>/8%CO<sub>2</sub>

way prior to analysis, in order to avoid contamination by any liquid left within the pores. The GD-OES operating conditions were 700 V and 20 mA.<sup>39</sup>

## Results and discussion

### Comparison of nitrocarburising response of various substrate materials

Figure 1 shows the diffusion of nitrogen and carbon into the surface of three different tool steel materials after 1 h of nitrocarburising. The left hand side of Fig. 1 (a–c) can be compared with the right hand side (d–f), which shows the same materials after treatment with ammonia and nitrogen gas only. Thus, the difference between the two diagrams is the extent of carbon diffusion due to the carbon activity imposed by carbon dioxide gas. It should be explained that 1 h treatments were chosen because the GD-OES instrument is only able to sputter ~60–90 µm into steel. The analysis ends when the material built up around the sputtered crater forms a short circuit with the anode. Thus, the exact length of analysis is subject to a certain amount of variation and cannot be controlled.

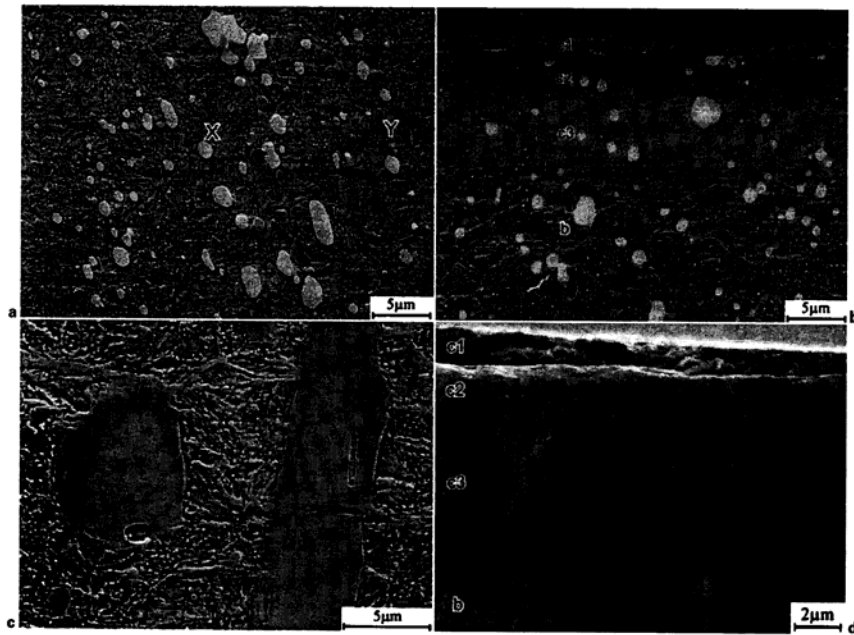
The various zones in the surface have been marked out using the notation 'a', 'b' and 'c', which refer to the substrate, diffusion zone and compound layer, respectively. Labels 'c1', 'c2' and 'c3', which further divide the compound layer into sublayers, will be encountered later.

Despite large differences in composition and microstructure, H13 and M2 exhibited a similar nitrocarburising response. D2 differed in that the overall penetration of nitrogen was less, and the diffusion zone–substrate (b–a) interface was more diffuse. This was due to the interaction of inward diffusing nitrogen with large carbides present in the D2 microstructure. Owing to the greater difficulty of nitrogen diffusion into the D2 substrate, nitrogen tended to accumulate in higher concentrations. In contrast, the similarity of H13 and M2, despite M2 containing significantly more

Table 2 Heat treatment procedures and hardness of tool steel substrates

Steel grade	Heat treatment procedure	HRC after heat treatment
P20 Plastic mould steel	Supplied in quenched and tempered condition	31 ± 1.0
H13 hot working die steel	Soak 1020–1030°C 45 min, quench in FB, single temper 580°C 1 h	48 ± 0.5
M2 high speed steel	Soak 1150°C 10 min, quench in FB, single temper 600°C	59 ± 1.0
D2 cold working die steel	Soak 1070°C 30 min, single temper 575°C, 1 h	55 ± 0.5





a M2 substrate ('X' and 'Y' carbides identified below); b M2 surface; c D2 diffusion zone showing conversion of large (Cr,Fe)<sub>7</sub>C<sub>3</sub> carbides to CrN (dark areas); d fractured H13 compound layer  
 3 SEM micrographs after 3 h N<sub>2</sub>/NH<sub>3</sub>/CO<sub>2</sub> treatment

carbon, is due to much of the carbon in M2 being locked up in alloy carbides which did not interact with nitrogen. The exact nature of these carbides will be discussed in more detail later.

Microhardness profiles after 3 h of nitrocarburising are shown in Fig. 2. Again, D2 exhibited a smaller diffusion zone, and a case-core interface that was quite diffuse. It was found that P20 differed markedly from the other three materials. The level of hardness accrued in the diffusion zone was significantly lower, and the curve flattened out very gradually. This was typical of a lower alloyed material. So far, these features are comparable with those observed by Ozbaysal *et al.* in their experiments on the different ion nitriding responses of the same substrate materials.<sup>15</sup>

As well as a large nitriding potential, the nitrocarburising atmosphere exerts a carburising potential on the surface. The amount of carbon that is absorbed from the gas phase is influenced by the carbon content of the substrate. Two carbon enrichment zones existed in all substrates, one at the c-b interface and a larger one at the b-a interface. The larger b-a carbon enrichment zone was due to carbon from the substrate being pushed ahead of the diffusion zone reaction front. The same effect after nitriding has also been revealed by other investigators using special etchants.<sup>19</sup> The smaller (c-b) carbon enrichment zone, however, forms as a result of several different processes.

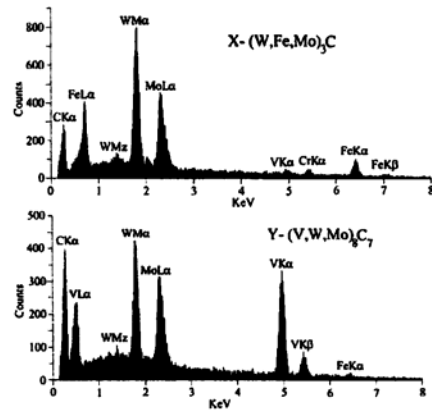
Carbon from the substrate is pushed ahead of the compound layer-diffusion zone interface in an analogous way to the b-a interface. Figure 1b shows

this smaller carbon peak in M2 steel in the absence of any gaseous carburising potential. It has also been detected by other authors after nitrocarburising of pure iron.<sup>40</sup> However, carbon built up to higher levels in this region when CO<sub>2</sub> was used. Hence, the source of carbon enrichment below the compound layer is both substrate carbon and carbon absorption from the atmosphere. Other investigators have claimed that carbon enrichment deep within the compound layer occurs owing to preferential absorption of carbon through pore channel surfaces at some depth below the outer specimen surface.<sup>41</sup> Furthermore, a certain amount of decarburisation occurs at the very surface during treatment, as evidenced by the carbon deficiency within the first several microns. Local decarburisation under the influence of N<sub>2</sub>/NH<sub>3</sub>/CO<sub>2</sub> or N<sub>2</sub>/NH<sub>3</sub> gas mixtures could occur by either of the following mechanisms



All the above factors contribute collectively to the shape of the carbon peak at the base of the compound layer.

In general, comparison of Fig. 1a-f shows that in higher carbon steels (M2 and D2) carbon diffusion into the steel during nitrocarburising with CO<sub>2</sub> affected mainly the compound layer and the region directly below it. There was no measurable increase in carbon concentration deeper within the diffusion zone in these steels. Carbon did, however, diffuse deeply into H13. Figure 1a shows that the carbon content of the whole



4 EDX spectra of carbides in M2 marked X (light) and Y (dark) in Fig. 3a

diffusion zone was raised by nitrocarburising. Microhardness profiling did not detect any measurable difference in hardness in the H13 treated without CO<sub>2</sub>.

#### Comparison of carbide conversion in M2 and D2

M2 and D2 substrates were nitrocarburised for 3 h using the following gas parameters: N<sub>2</sub>/25%NH<sub>3</sub>/8%CO<sub>2</sub>. The M2 substrate structure after treatment (Fig. 3a) exhibited a martensitic matrix and two distinct carbides: one dark and one light. EDX analysis (Fig. 4) showed that the light carbides were rich in iron, tungsten and molybdenum, while the dark carbides contained vanadium, tungsten and molybdenum. XRD (Fig. 5) identified them as (W, Fe, Mo)<sub>3</sub>C and (V, W, Mo)<sub>8</sub>C<sub>7</sub>.

Earlier work on plasma nitriding of M2 found that the tungsten containing carbides were stable, i.e. they remained untransformed after nitrogen impregnation of the surface.<sup>15</sup> However, in the present investigation, some conversion of (W, Fe, Mo)<sub>3</sub>C was observed within the compound layer, where the nitrogen concentration reached very high levels. At least two hexagonal tungsten nitrides could be identified in Fig. 5a and b. These were W<sub>2</sub>N (ref. 42) and a ternary iron tungsten nitride FeWN<sub>2</sub>.<sup>43</sup> A third tungsten nitride, W<sub>4-6</sub>N<sub>4</sub>,<sup>44</sup> may also have been present, although many peaks were obscured. Nevertheless, throughout the diffusion zone the carbides were indeed untransformed, in accordance with Ozbaysal *et al.*<sup>15</sup> (Fig. 5c). This explains the 'locking up' of carbon in M2, which caused it to behave similarly to H13 as regards layer growth kinetics.

The D2 substrate contained large chromium carbides, which were identified as (Cr, Fe)<sub>7</sub>C<sub>3</sub> (Fig. 5g). In contrast to the tungsten and molybdenum containing carbides in high speed steel, these iron–chromium carbides transformed readily to CrN both in the diffusion zone and in the compound layer. However, owing to their size, the complete transformation of carbides was difficult. Figure 3c shows two partially transformed carbides in the diffusion zone. The CrN areas etched darker than the surrounding untransformed carbide. The transformation front had passed through the area shown on this micrograph a long time before the end of treatment. This explains the

diffuseness of the diffusion zone–substrate interface, as discussed above.

Optical micrographs of D2 treated with N<sub>2</sub>/NH<sub>3</sub> and N<sub>2</sub>/NH<sub>3</sub>/CO<sub>2</sub> mixtures are shown in Fig. 6d and e. The diffusion zone etched heavily with nital etching: the substrate microstructure was not revealed unless much longer etching times were used. For easier observation of the converted carbides, therefore, an unetched micrograph is also shown (Fig. 6f). It was found that the depth of carbide transformation was about half to two-thirds the total depth of the diffusion zone. This ratio was independent of total nitrocarburising time. It also did not alter if CO<sub>2</sub> or no CO<sub>2</sub> were used, which was not surprising, given that carbon from the treatment atmosphere did not penetrate far into the diffusion zone of D2. Complete conversion of the larger carbides only occurred near the surface and after long treatment times.

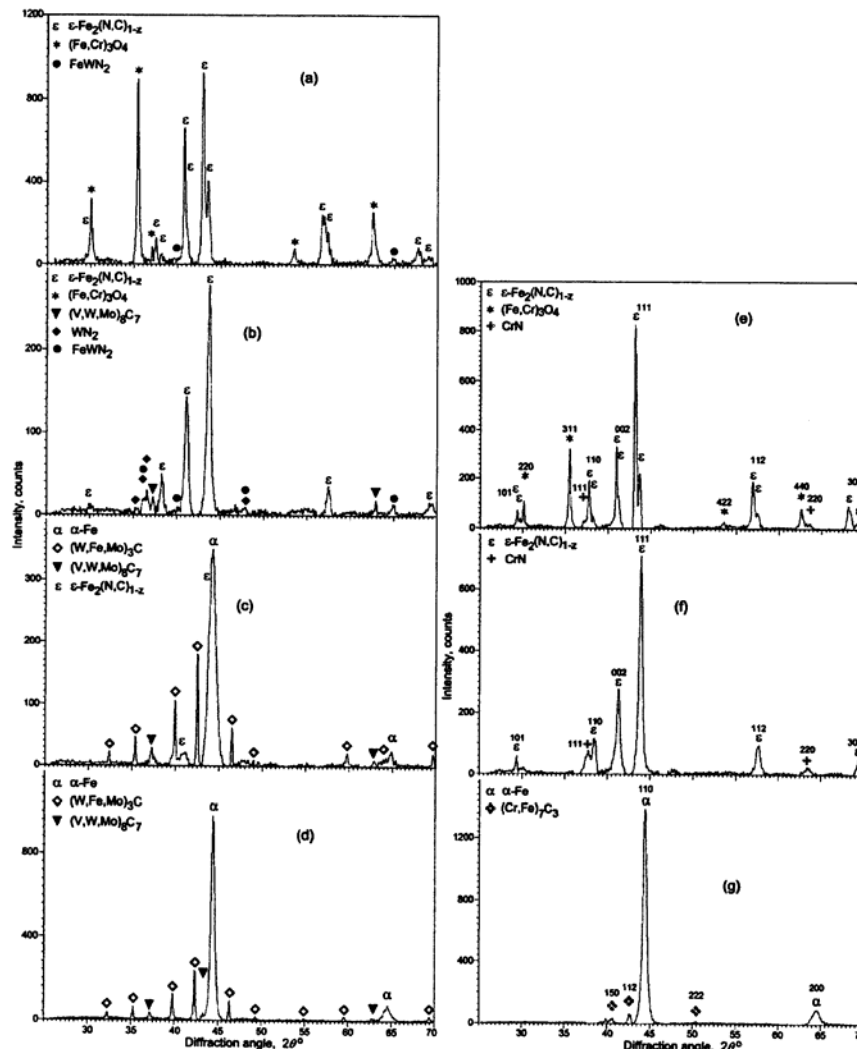
#### Detailed characterisation of compound layer formed on M2 high speed steel

It has been shown that, during nitrocarburising, carbon enrichment affects mainly shallower regions in high carbon materials and may diffuse deeper into other substrates, such as H13. However, the use of carbon dioxide as the carbon bearing component during nitrocarburising has its most dramatic influence on the shape of the compound layer. This is due, in particular, to a higher oxygen potential when CO<sub>2</sub> is used, which has a catalytic effect on epsilon carbonitride nucleation and/or growth. This will now be explored further, and the results can be compared with other types of compound layers formed with N<sub>2</sub>/NH<sub>3</sub> and N<sub>2</sub>/NH<sub>3</sub>/natural gas mixtures (discussed later). High speed steel was chosen as a suitable, representative substrate material, owing to its variety of alloying elements. M2 contains all the major elements present in tool and alloy steels.

After treatment with N<sub>2</sub>/NH<sub>3</sub>/CO<sub>2</sub>, the M2 compound layer contained a distinct sublayer pattern, which in Fig. 3b has been broken down into three layers: c1, c2 and c3. In fact, the same basic three layered pattern was seen in all materials treated using CO<sub>2</sub>. Figure 3b shows that the carbides ended at the interface between c1 and c2. No carbides could be seen in the surface layer c1. Some carbides had been cut through at the c1–c2 interface during the grinding process before treatment. Thus, the c1–c2 interface could be clearly identified as the surface of the sample at the beginning of treatment.

The nitrocarburised M2 surface was also analysed using the GD-OES spectrometer. The resulting depth profile into the surface (Fig. 7) has been displayed on two sets of axes – the top graph shows the elements N, C, O and Fe, while the bottom graph shows Cr, Mo, V, W and Ni. Both axes have the same horizontal scale.

The fully dense sublayer c3 formed the majority of the compound layer. The conventional porous zone c2, occupying 1.5–4 μm from the surface, had a dull grey appearance under the optical microscope. A further sublayer c1 found at the very surface (initial ~1.5 μm in Fig. 7) was similar in some respects to scale: it was highly porous (Fig. 3b), and it contained a large amount of oxygen (Fig. 7). In contrast, it appeared white and reflective under the optical microscope after polishing, not grey (see Fig. 6e and f for an example in D2).



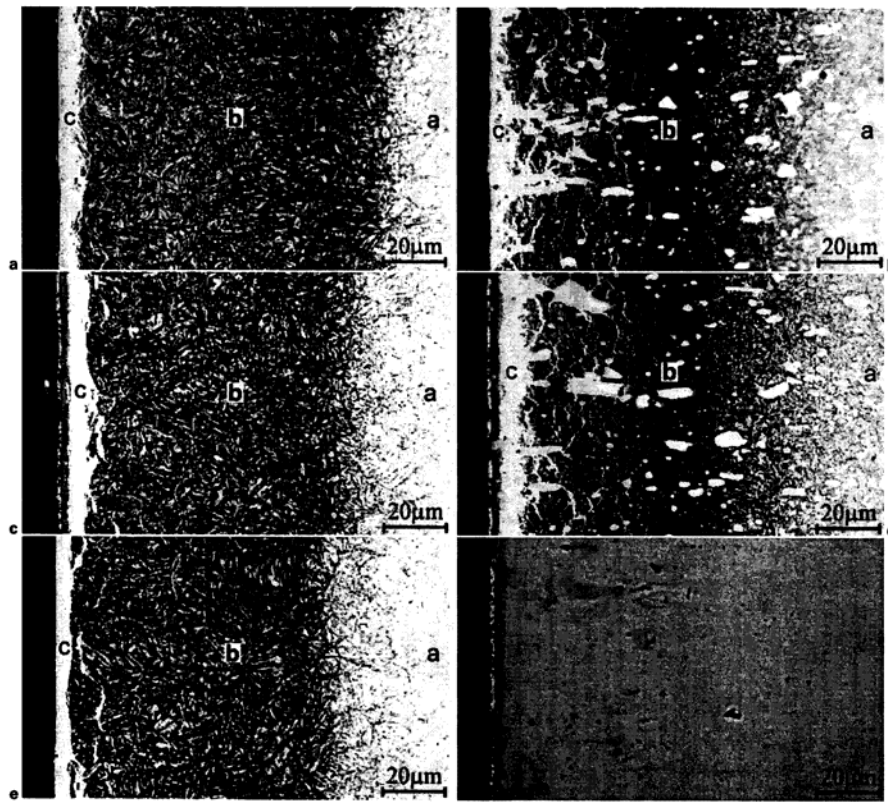
a surface; b 7 μm below surface; c 35 μm below surface; d substrate; e surface; f 3 μm below surface; g substrate  
 5 Phase transformations at various depths into a-d M2 and e-g D2 surfaces after 3 h of nitrocarburising, N<sub>2</sub>/NH<sub>3</sub>/CO<sub>2</sub>

From Fig. 7, it is clear that the composition of the c1 layer was not uniform. Towards the surface, oxygen was the dominant element. However, the matching peaks in Fe and N within c1 also suggest the presence of an iron nitride. This was confirmed by XRD examination of the surface, which yielded double epsilon nitride peaks (Fig. 5a). When the c1 layer was ground off, and XRD was re-performed on the underlying surface, only one set of epsilon peaks remained (Fig. 5b). This indicated that the higher lattice parameter epsilon nitride signal came from the c1 layer. The relative peak positions after different treatment times was also noted, and it was found that the lattice parameters of c1 decreased with time. In contrast, the lattice parameters of the remaining ε-phase material stayed relatively constant, therefore the distance 2θ between the dual peaks tended to get

smaller. It is known that the epsilon lattice parameters increase with increasing stoichiometric ratio of nitrogen to iron atoms.<sup>45</sup> Twin epsilon peaks were also seen on D2 (Fig. 5e).

The c1 sublayer was also observed by Pietzsch *et al.*,<sup>46</sup> who referred to it as the 'cover layer'. They showed that the thickness of the cover layer was proportional to the square root of the treatment time, indicating diffusion controlled growth. A strong relationship was found between the presence of porosity in the compound layer and the occurrence of the cover layer.

A model for the porous zone and cover layer development can now be proposed. Pores form in c2 as the nitrogen concentration builds up. This is a result of the recombination of dissolved nitrogen to form molecular nitrogen. At the same time, the cover layer



a  $N_2/NH_3$ ; b  $N_2/NH_3/8\%CO_2$ ; c  $N_2/NH_3/10\%$  natural gas; d  $N_2/NH_3$ ; e  $N_2/NH_3/16\%CO_2$ ; f  $N_2/NH_3/CO_2$ , unetched  
6 Effect of carbonaceous gas on a-c H13 and d-f D2 microstructure

forms by the outward diffusion of iron. Its thickness increases with increasing treatment time. Iron diffusion across the c1-c2 interface is driven by the oxygen potential at the surface. The formation of pores in c2 may assist this process, because loss of nitrogen to the atmosphere by recombination creates local areas that are rich in iron. As the porous oxide layer thickens, conditions at the c1-c2 interface may become more reducing, and transformation of iron oxide to iron nitride results. Substitutional diffusion of iron within c1 is required for this to occur, which explains the initial saturation of nitrogen in the  $\epsilon$ -nitride formed.

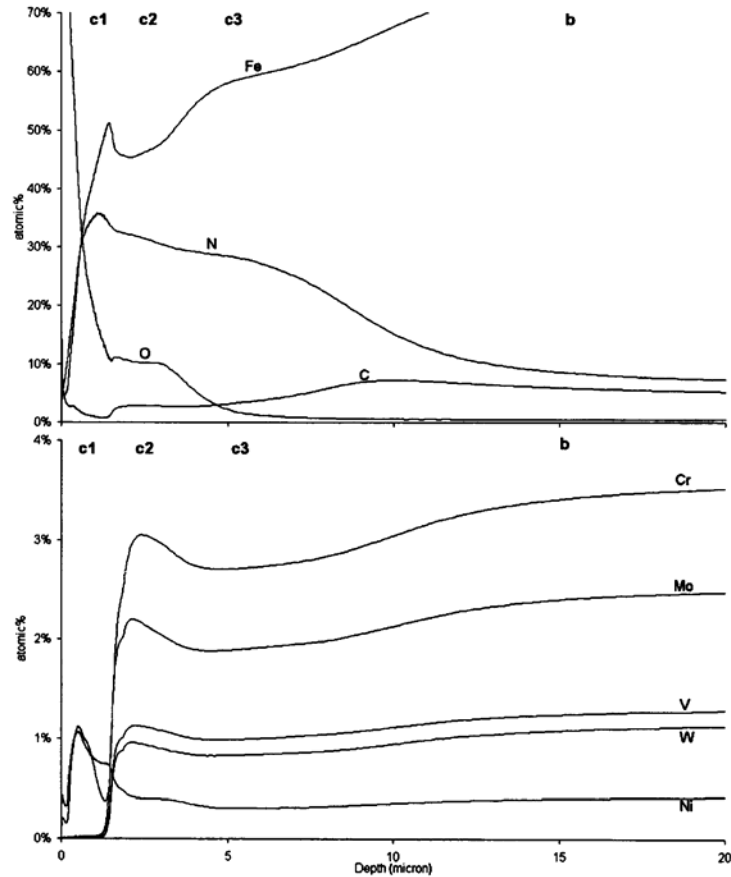
Porosity also creates a large amount of free surface area in c2 that is exposed to the oxidising atmosphere. Thus, the oxygen detected in this region was as high as 10 at.-%. There appears to have been a certain amount of diffusion of alloying elements towards the porous region from deeper within the compound layer. Cr, Mo, V and W were all driven to free surfaces owing to the oxidising potential. In steels with fewer alloying elements, such as H13, the same effect was seen, but only involving those alloying elements that were present in the substrate material.  $Me_3O_4$  in c2 may have been thick enough to close in the pores fully: an important effect, considering the supposed lubricant retention capability of the porous zone. Figure 3d shows the compound layer on H13 prepared by brittle fracture,

rather than mounting and polishing, so as to preserve the porosity. There is little evidence of open pores within the c2 region of this micrograph. While porosity in H13, M2 and D2 was extremely fine, and individual pores were not visible, a micrograph of a P20 compound layer is shown in Fig. 9c, which shows a coarser brand of porosity. The relative thicknesses of the c1, c2 and c3 layers also varied from material to material.

One final observation on the M2 elemental depth profile (Fig. 7) is the small peaks in Ni, Cr and Al within the first micron of the surface (aluminium is not included on this graph, but was present). Iron was the only metallic element that diffused over the c1-c2 interface, while these elements were detected within the c1 sublayer. They were due to contamination picked up by abrasive contact with the powder in the bed. Examination of the oxide layer on mild steel formed during the same treatment showed that the same elements, which were not present in the substrate, were also deposited on this material.

#### Effect of carbon absorption on nitrogen diffusion and use of natural gas

Figure 6a-c shows the typical microstructures produced after nitrocarburising H13. H13 contained a much finer dispersion of carbides than M2 or D2, which were not easily seen under the optical microscope. They were also



7 Depth profile of M2 from surface through to diffusion zone; horizontal scales are identical, vertical scales differ

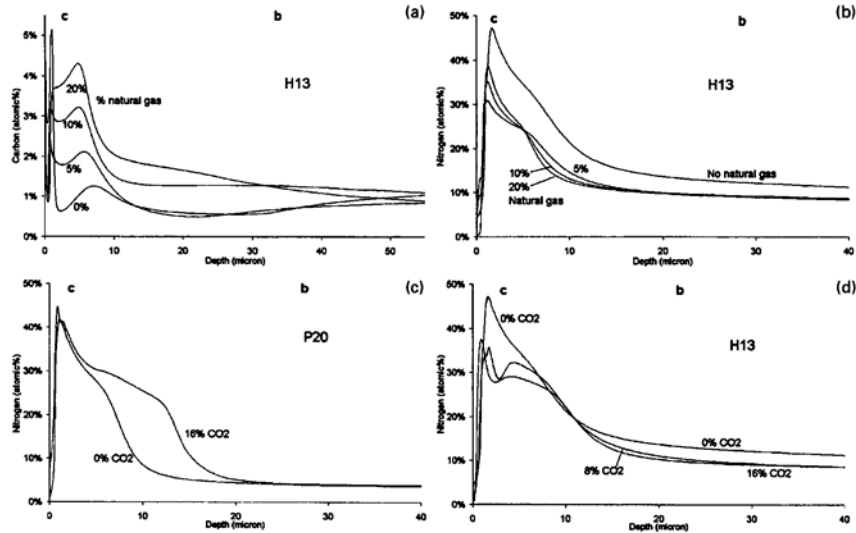
not detected by XRD. However, they could be expected to contain chromium, and to dissolve readily or transform directly to  $\text{CrN}$ , as has been commonly found with nitriding of H13.<sup>15,16</sup>

For a given substrate material, the choice of carbon bearing gas or its absence from the treatment atmosphere most of all affected the type of compound layer produced by the nitrocarburising treatment. H13 compound layers, just like those on M2 and D2, were dominated by  $\epsilon$ -carbonitride, while  $\gamma'$  was not detected.  $\text{CO}_2$  containing atmospheres produced thicker compound layers on H13, as well as on the other materials investigated. Owing to this rapid compound layer development, the  $\text{CO}_2$  layers were also the most porous. Only the compound layers formed with  $\text{CO}_2$  exhibited the characteristic three sublayer structure. The compound layer formed with  $\text{N}_2/\text{NH}_3$  was the most dense on H13 (Fig. 6a). The external appearance of the  $\text{N}_2/\text{NH}_3$  samples was brighter, visibly less oxidised than the others.

In contrast, compound layers produced with natural gas were thinner than the other types of compound layers (Fig. 6c). They were less prone to porosity than those formed in  $\text{N}_2/\text{NH}_3/\text{CO}_2$  mixtures (although

porosity was also a function of substrate composition and treatment time). Natural gas was found to be much more effective at raising the carbon concentration of the treated surface than was carbon dioxide. Figure 8a shows the influence of natural gas level on the carbon profile in H13. The carbon uptake showed a strong correlation with the level of natural gas used, whereas increasing the  $\text{CO}_2$  level from 8% to 16% had no apparent effect on any of the diffusion profiles. Most importantly, however, local decarburisation at the surface did not occur when natural gas was used. Up to 4 wt-% carbon was reached using 20% natural gas in the inlet mixture. Thick grain boundary cementite formed below the compound layer, owing to the enrichment of carbon in this area too. In Fig. 6, grain boundary cementite just beneath the compound layer was white against the surrounding diffusion zone.

It will now be shown that these differences in the level of carbon absorption also had an effect on the shape of the nitrogen profile. Figures 8b–d show nitrogen depth profiles up to 40  $\mu\text{m}$  into H13 with 0–20% natural gas, P20 with 0–16%  $\text{CO}_2$  and H13 with 0–16%  $\text{CO}_2$ , respectively. Increased carbon occupancy reduced the overall concentration of nitrogen, in particular with the very



a H13,  $N_2/NH_3$ , 3 h; b H13,  $N_2/NH_3/10\%$  natural gas, 3 h; c P20,  $N_2/NH_3/8\%CO_2$ , 6 h  
 8 a GD-OES carbon and b-d nitrogen depth profiles showing effect of carbonaceous gas

high carbon levels found in the natural gas treated samples. Carbon also reduced the diffusivity of nitrogen into the steel. Optical micrographs of H13 show that the diffusion zone was deepest in the  $N_2/NH_3$  sample, shallower in the  $N_2/NH_3/CO_2$  sample, and shallowest for  $N_2/NH_3$ /natural gas, in order of increasing carbon absorption. This behaviour, however, also depended on the particular substrate under investigation. In D2, for instance, this difference in nitrogen diffusivity was less, while in P20, no difference between the diffusion zone nitrogen levels was found. This was also in accordance with the extent of carbon uptake as a function of substrate material, as discussed earlier.

The influence of carbon on nitrogen diffusivity also affected the sharpness of the interface between the compound layer and the diffusion zone: note the trend in Fig. 5b for natural gas. Samples treated without any carbonaceous component displayed a very broad transition from compound layer to diffusion zone. Figure 9a shows a more detailed view of the surface microstructure on the 25% $N_2/NH_3$ H13 sample. Note that owing to the slightly different chemistry of this 'white layer', some etching with nital did occur, and the underlying martensite lath microstructure was revealed. It is clear that formation of the epsilon phase in the c-b interfacial region is highly influenced by the tempered martensite microstructure, and that it occurred at favourable sites at prior lath boundaries. No clear boundary between compound layer and diffusion zone was evident. Instead, numerous pockets of untransformed material remained behind the transformation front. This contrasted with the  $N_2/NH_3$ /natural gas compound layer, where carbon ahead of the transformation front prevented easy diffusion of nitrogen into the diffusion zone, which meant more complete transformation to epsilon carbonitride at the c-b interface, and a sharper transition in the nitrogen curve. Again, this varied from material to material, and there is a well

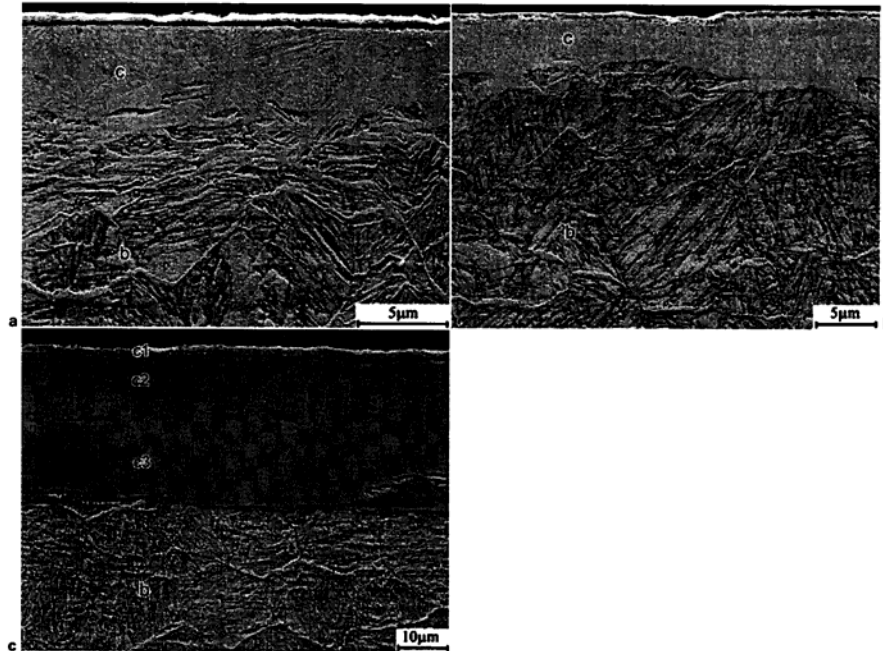
defined transition between compound layer and diffusion zone in P20 treated with  $CO_2$  (Fig. 9c) but not in M2 (Fig. 3b).

Finally, it is noted that nitrogen activities imposed by the various treatments were not constant and would have had some effect on the nitrogen profiles and diffusion depths. Addition of carbon dioxide to the  $N_2/NH_3$  gas mixture at constant partial pressure of ammonia actually has the effect of slightly increasing the nitrogen activity, owing to hydrogen consumption in reactions 3 and 4. Vogel<sup>47</sup> measured the change in nitrogen activity caused by  $CO_2$  addition from ir analysis of the exit gas, and indeed detected an increase in  $a_N$ . Addition of natural gas to  $N_2/NH_3$ , in contrast, reduces  $a_N$ . Therefore, this must be taken into more serious consideration, because it runs with the trend in diffusion depth seen in Fig. 6. However, the results also vary considerably, depending on the substrate material chosen and the extent of carbon absorption in each, indicating that any drop in  $a_N$  due to natural gas addition played a smaller role than the microstructural effects.

### Comparison of surface properties

Diffusion profiles and microstructures were investigated using  $N_2/NH_3$ ,  $N_2/NH_3/CO_2$  and  $N_2/NH_3$ /natural gas mixtures. Now the mechanical properties resulting from these three basic types of treatment will be compared, although a more thorough investigation involving wear testing is published elsewhere in this journal.<sup>48</sup>

The surface properties of nitrocarburised samples were compared by hardness indentations on the treated surface. Hardness tests were performed after a brief polish with 1  $\mu m$  diamond paste to produce a reflective (but not necessarily bright) surface. Optical examination of cross-sections after polishing confirmed that  $<1 \mu m$  had been removed, so that even the c1 layer remained. The surface hardness was then measured using 200 g



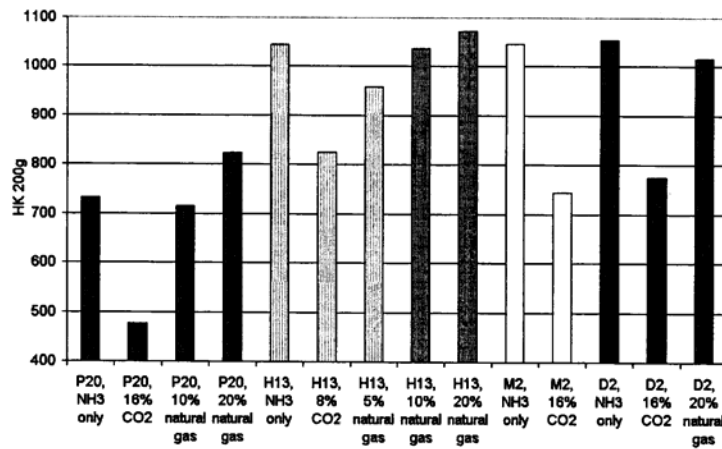
9 Effect of material and process parameters on compound layer morphology and c-b transition region

Knoop microindentations (Fig. 10). Indenter penetration was typically 1.7–1.9 µm.

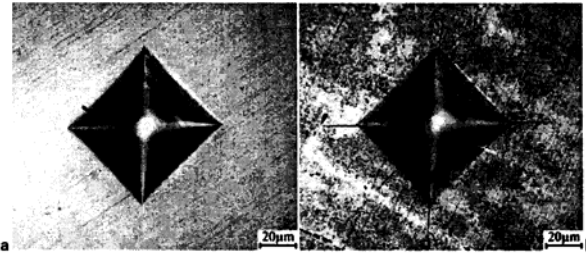
The surface hardness of all materials nitrocarburised with carbon dioxide was significantly lower than with other gas mixtures. This was due to the effect of porosity collapsing under the load. Therefore, although the real hardness of the dense compound layer material was not lower, this would have been the effective hardness of the surface seen in practice. The N<sub>2</sub>/NH<sub>3</sub> mixture, on the other hand, produced a nearly fully dense layer, which supported the load effectively. Natural gas treatments also generated some porosity, and suffered some loss in

surface hardness as a result. However, the porosity was not as severe as when CO<sub>2</sub> was used, particularly on the higher alloyed substrates. It was found that as the level of natural gas was increased, and the compound layers become increasingly enriched with carbon, the hardness improved accordingly.

Porosity also resulted in embrittlement of the surface; 5 kg Vickers indentations on the polished surfaces were made, and the extent of cracks extending from the corners of the indentation were used as a measure of the relative surface brittleness (Fig. 11). The results are summarised in Table 3, rating the degree of fracture on



10 200 g Knoop microhardness tests on treated polished surfaces

a N<sub>2</sub>/NH<sub>3</sub>; b N<sub>2</sub>/NH<sub>3</sub>/8%CO<sub>2</sub>

### 11 Examples of two 5 kg Vickers hardness tests on treated polished H13 surfaces

a scale of 0–3. N<sub>2</sub>/NH<sub>3</sub> gas mixtures proved to generate more ductile surfaces than the other two treatments. In P20, the difference between the three treatments was more difficult to ascertain, probably owing to the ready occurrence of porosity under any conditions in this material. Overall, it can be said that the 3 h N<sub>2</sub>/NH<sub>3</sub> treatment resulted in an excellent combination of hardness and ductility on H13 and M2 and probably also on D2.

## Conclusions

1. It is generally known that the carbonaceous gas in nitrocarburising plays an important role in determining the compound layer characteristics. However, it also influences the carbon enrichment zone at the compound layer–diffusion zone interface, contributing in tool steels to the coarsening of grain boundary cementite. In H13, carbon was found to diffuse deeper, affecting the whole diffusion zone.

2. Carbon absorption affects nitrogen diffusivity in the diffusion zone. However, no measurable change in hardness was observed in these substrates due either to carbon diffusion or to change in the nitrogen profile.

3. When the nitrocarburising atmosphere has a high oxygen potential, such as when CO<sub>2</sub> is used, a thick compound layer is produced, with three clearly discernable sublayers. The top, cover layer forms owing to diffusion of iron to the surface, formation of iron oxide and partial reduction back to iron nitride.

4. The advantage of porosity in the compound layer on tool steel substrates is questionable, owing to its very fine nature and the observation that the entire pore volume is apparently closed in by Me<sub>3</sub>O<sub>4</sub>.

5. Nitrocarburising with natural gas is cheaper and on tool steels, produces harder, less brittle and oxidised compound layers than does carbon dioxide. Decarburisation does not occur at the outer surface, so the carbon content of the compound layer was able to reach high levels. Increasing partial pressure of natural

gas results in further carbon absorption. Other hydrocarbon based gases, such as propane or liquid petroleum gas, may also have the same property.

6. For certain applications, a 3 h treatment without carbonaceous gas produces an excellent combination of hardness and ductility. Embrittlement due to porosity is prevented, as well as the development of grain boundary Fe<sub>3</sub>C in the diffusion zone, which can otherwise form networks, especially near corners. Carbon free treatment could be an excellent choice for a high speed cutting tool, for example, where brittleness must be avoided. The high carbon content of the substrate means that the ε-phase is stabilised and little carbon would be absorbed from the gas phase if carbonaceous gas were used.

## References

1. H. J. Grabke: *Ber. Bunsenges. Phys. Chem.*, 1968, **72**(4), 533–541.
2. H. J. Grabke: *Ber. Bunsenges. Phys. Chem.*, 1968, **72**(4), 541–548.
3. G. Engelhardt and C. Wagner: *Z. Phys. Chem. B*, 1932, **18**(6), 369–379.
4. T. Bell and S. Y. Lee: in 'Heat treatment '73'; 1973, London, The Metals Society.
5. C. Dawes: *Heat Treat. Met.*, 1990, **17**(1), 19–30.
6. K. Bennett, Q. Weir and J. Williamson: *Heat Treat. Met.*, 1981, **8**(4), 79–81.
7. C. Dawes, D. F. Tranter and C. G. Smith: *Met. Technol.*, 1979, **6**(9), 345–353.
8. G. Wahl: *Mater. Sci. Forum*, 1994, **163–165**, 309–314.
9. N. Krishnaraj, P. B. Srinivasan, K. J. L. Iyer and S. Sundaresan: *Wear*, 1998, **215**, 123–130.
10. C. T. Kwok, K. I. Leong, F. T. Cheng, and H. C. Man: *Mater. Sci. Eng.*, 2003, **A357**, 94–103.
11. K. Keller: *Plastverarbeiter*, 1972, **23**(1), 1–6.
12. E. Mitchell and C. Dawes: *Met. Treat. Drop Forg.*, 1964, **31**, 3–16, 49–58, 88–96, 195–200, 226–234, 265–276.
13. J. C. Gregory: *Met. Form.*, 1968, **35**, 229–238, 240.
14. J. Slycke and L. Sproge: *Surf. Eng.*, 1989, **5**, 125–140.
15. K. Ozbaysal, O. T. Inal and A. D. Romig: *Mater. Sci. Eng.*, 1986, **78**, 179–191.
16. O. Salas, J. Oseguera, N. Garci and U. Figueroa: *J. Mater. Eng. Perform.*, 2001, **10**(6), 649–655.
17. J. L. Albarran, J. A. Juarez-Islas and L. Martinez: *Mater. Lett.*, 1992, **15**, 68–72.
18. V. A. Phillips and A. U. Seybolt: *Trans. Metall. Soc. AIME*, 1968, **242**(Dec), 2415–2422.
19. S. Mridha and D. H. Jack: *Met. Sci.*, 1982, **16**, 398–404.
20. B. Edenhofer: *Heat Treat. Met.*, 1974, **1**(2), 59–67.
21. J. Slycke, L. Sproge and J. Agren: *Scand. J. Metall.*, 1988, **17**, 122–126.
22. H. Du: *J. Phase Equilibria*, 1993, **14**(6), 682–693.
23. T. Bell: *Heat Treat. Met.*, 1975, **2**(2), 39–49.
24. C. Dawes, D. F. Tranter and C. G. Smith: *Heat Treat. Met.*, 1980, **7**(1), 1–4.
25. T. Bell, B. J. Birch, V. Korotchenko and S. P. Evans: in 'Heat treatment '73'; 1973, London, The Metals Society.

**Table 3** Visual inspection of cracking around 5 kg Vickers indentations: 0=no cracks, 1=minor cracks, 3=extensive cracks

Material	NH <sub>3</sub> only	NH <sub>3</sub> +CO <sub>2</sub>	NH <sub>3</sub> +20% natural gas
P20	2	3	2
H13	0	3	2
D2	1	3	1

26. T. Rose and A. Manriquez: Proc. 16th Conf on 'Heat treating'; 1996, Cincinnati, OH, ASM.
27. G. J. Tymowski et al.: 'Nitreg-ONC—a new, improved anti-corrosion treatment', Technical Paper, Nitrex Metal Inc., St Laurent, Quebec, Canada, 1999.
28. L. Z. Zhang et al.: 6th Int. Congr. on 'Heat treatment of metals'; 1988, Chicago, ASM.
29. G. Wahl and S. Alwart: Proc. 16th Conf on 'Heat treating'; 1996, Cincinnati, OH, ASM.
30. P. C. King, R. Reynoldson, A. Brownrigg and J. M. Long: *J. Mater. Eng. Perform.*, 2004, **13**(4), 431–438.
31. P. C. King, R. W. Reynoldson, A. Brownrigg and J. M. Long: *Surf. Coat. Technol.*, 2004, **179**(1), 18–26.
32. C. Dawes, D. F. Tranter and R. W. Reynoldson: in 'Heat treatment '73'; 1973, London, The Metals Society.
33. U. Ebersbach, S. Friedrich, T. Nghia and H.-J. Spies: *Härt.-Tech. Mitt.*, 1991, **46**, 339–349.
34. C. Leroux: *Trait. Therm.*, 1985, **196**, 29–35.
35. B. Prenosil: *Härt.-Tech. Mitt.*, 1965, **20**(1), 41–49.
36. K. E. Moore and D. N. Collins: *Heat Treat. Met.*, 1996, **23**(4), 95–98.
37. P. C. King, R. Reynoldson, A. Brownrigg and J. M. Long: 3rd Int. Conf. on 'Advanced materials processing'; 2004, Melbourne, Australia, IMEA.
38. The Victorian Energy Networks Corporation: [www.vencorp.com.au](http://www.vencorp.com.au).
39. R. Payling, D. G. Jones, and A. Bengtson (eds.): 'Glow discharge optical emission spectrometry'; 1997, Chichester, John Wiley.
40. H. C. F. Rozendaal, P. F. Colijn and E. J. Mittemeijer: in 'Heat treatment '84'; 1984, London, The Metals Society.
41. M. A. J. Somers and E. J. Mittemeijer: *Surf. Eng.*, 1987, **3**(2), 123–137.
42. V. I. Khitrova and Z. G. Pinsker: *Kristallografiya*, 1960, **5**, 711.
43. D. S. Bem, C. M. Lampe-Onnerud, H. P. Olsen and H.-C. zur Loye: *Inorg. Chem.*, 1996, **35**(3), 581–585.
44. V. I. Khitrova and Z. G. Pinsker: *Kristallografiya*, 1958, **3**, 545.
45. M. A. J. Somers and E. J. Mittemeijer: *Metall. Mater. Trans.*, 1995, **26A**, 57–74.
46. S. Pietzsch and S. Bohmer: *Mater. Sci. Forum*, 1994, **163–165**, 259–264.
47. W. Vogel: 6th Int. Congr. on 'Heat treatment of metals'; 1988, Chicago, ASM.
48. P. C. King, R. W. Reynoldson, A. Brownrigg and J. M. Long: *Surf. Eng.*, 2005, **21**(2), 99–106.